Integrated Master in Chemical Engineering

Preparation and Evaluation of Material Properties of Biofilms from Spruce Xylan

Master Thesis

CHALMERS

Departamento f Chemical and Bilogical Engineering

U. PORTO
FEUP FACULDADE DE ENGENHARIA
UNIVERSIDADE DO PORTO

Departamento f Chemical Engineering

Student:	**Supervisors in Chalmers:**
Ana Margarida da Cunha Gonçalves	Aase Bodin
	Paul Gatenholm

Julho de 2011

Acknowledgements

I would like to express my gratitude to everyone in general who were involved in my thesis or facilitated my work in one way or another, or on the other hand, were concerned with my thesis work. I would like to thank in particular:

- My supervisor, Aase Bodin, whose knowledge, understanding and patience, helped me considerably in my project over the past six months. I appreciate your assistance in all levels of the research project and her contribution in writing report. I also want to thanks for your patience with my English.
- My examiner, Paul Gatenholm, first for giving me the opportunity to do my thesis with him and second for his support and enthusiasm.
- My first friend in Sweden, Guillermo, for his help and teachings. It was very nice meeting you.
- My parents, Helena and Manuel, without their education and advices I would not be the person that I am today. I thank them for their efforts and encouragement to support me in my course. You are everything to me.
- My boyfriend, Luís, for your understanding to accept my Master’s at 3 500 km from Portugal and the love and courage you gave me during this time.

It is a pleasure to thank those who made this thesis possible and I want also say that it was great fun working with everyone.

I would like to show my gratitude to all of my professors from FEUP that teach me to be a Chemical Engineer. I am indebted to my closed colleagues (Sofia, Isabel, Cassilda) from my course to support me during these 5 happy years. I owe my gratitude also to my few but true friends (Tita, Claudia, Cátia e Bárbara) for your friendship and support.

Abstract

The climate change and scarcity of natural resources have increased the global awareness so it is necessary to reduce our carbon footprint by introducing more sustainable materials. Today there are effective processes for isolating cellulose for paper products. At the same time, a number of other components, such as hemicelluloses and lignin, are destroyed during isolation process. There are research results indicating that these products may be seen as valuable raw materials in the future.

Hemicelluloses are a group of heteropolysaccharides present in plant cell walls, fresh water plants and in some seaweed. The composition and structure of hemicelluloses differ depending on the source and type of plant. Xylans are the most abundant hemicelluloses in hardwood and annual plants. Their backbone is composed of β-(1→4)-linked-D-xylopyranose units. Depending on the source, xylans can be substituted with different side groups.

Xylans have many interesting properties and have been evaluated in various application areas e.g. as barrier material for food packages, matrix material in composites and hydrogels for biomedical purposes just to mention a few. The foremost interesting properties of xylan as a barrier material are its low oxygen barrier and its good mechanical properties in terms of strength and flexibility. The main obstacle though is its high hygroscopic nature resulting in limited success in moisture environments.

Films based on arabinoglucuronoxylan extracted from Norway spruce were prepared by water casting. Plasticizer was added in different concentrations to produce a variation in material properties. The sugar composition confirmed that the spruce xylan was composed of arabinose, glucuronic acid and xylose in a ratio of 1:2:11, respectively. The molar mass of the sample was 12 780 g/mol. Pure xylan film was totally amorphous whereas the plasticized films showed small peaks of crystallinity on X-ray diffractrogram, representing crystallized sorbitol. The average stress at break for the non plasticized films was 55 MPa, strain at break 2.7 % and Young’s Modulus 2 735 MPa. The addition of sorbitol causes a reduction in strength and stiffness, as expected. The DMA showed that the non plasticized films softened at 80% RH. According to moisture sorption isotherm the arabinoglucuronoxylan is highly hydroscopic. At 100% RH, the water content was 125%. The films showed low oxygen permeability (0.12-0.17 cm^3 μm m^{-2} d^{-1} kPa^{-1}) and thus have a potential application in food packaging.

Table of Contents

Notation

A	Cross area section
a,b,c	Lattice planes
A_2	Second osmotic virial coefficient
A_A	Amorphous area
A_C	Crystalline area
c	Sample concentration
d_{hkl}	Spacing between atomic planes
E	Young’s Modulus
E*	Complex modulus
E’	Storage modulus
E’’	Loss modulus
F	Force applied
G	Shear modulus
h,k,l,	Miller indexes
K	Optical parameter
L	Initial length
l	Thickness of polymeric barrier
M_w	Weight average molecular weight
n	Integer that defines the order of diffraction
n_0	Refractive index of the solvent
N_A	Avogadro’s number
$P(\theta)$	Function that describes the angular dependence of scattered light
R_θ	Intensity of light scattering at the angle θ
t	Time
X_C	Rate of crystallinity
γ	Shear strain
δ	Phase difference
ΔL	Increment of length
Δm_{gas}	Quantity of permeant
ΔP	Partial pressure difference

Δt	Duration of permeance
ε	Strain
ε_0	Amplitude in a sinusoidal strain
λ_0	Wavelength of the incident light
σ	Stress
σ_0	Amplitude in a sinusoidal stress
τ	Shear stress
ω	Angular frequency

Abbreviations

Ac	Acetyl group
AcGGM	o-acetyl-galactoglucomannans
Ara*f*	Arabinose or Arabinofuranosyl
CMC	Carboxymethylcellulose
DMA	Dynamic Mechanical Analysis
DP	Degree of Polymerization
EB	Electron bean
Gal*p*	Galactose or Galactopyranosyl
Glc*p*	Glucose or Glucopyranosyl
Glc*p*A	Glucuronic acid or Glucuronic acid unit in pyranose form
HIV	Human immunodeficiency virus
HMBC	Heteronuclear Multiple Bond Correlation
HPAE	High Performance Anion Exchange
HSQC	Heteronuclear Single Quantum Coherence
LCC	Lignin Carbohydrate Complex
LS	Light scattering
Man*p*	Mannose *or* Mannopyranosyl
Me	Methyl
NMR	Nuclear Magnetic Resonance
NOESY	Nuclear Overhauser Effect Spectroscopy
OP	Oxygen Permeability
OPC	Oxygen Permeability Coefficient
OTR	Oxygen Transmission Rate
PAD	Pulsed Amperometric Detection
RH	Relative Humidity
RI	Refractive index
SEC	Size Exclusion Chromatography
TOCSY	Total Correlation Spectroscopy
UV	Ultraviolet
WAXS	Wide Angle X-ray Scattering

WVP	Water vapour permeability
WVS	Water Vapour Sorption
Xyl*p*	Xylose or Xylopyranosyl

1. Introduction

Packaging material affects our everyday life and comprises approximately 66 % of the post-consumer plastic waste in Europe [1]. The increased social and environmental consciousness in conjunction with strict regulations on pollutants and disposal of waste products put pressure on the industries to find new solutions to improve recycling streams and reduce the consumption of fossil fuels [2]. The most common barrier materials in today's food packages are either aluminum or various synthetic plastics [3]. Commercialization of bioplastics, biopolymers from renewable resources, are on its way and may serve as a new environmental source for barrier material that may also reduce the solid waste by being biodegradable [2].

Today bioplastics represent less than 0.25 % of the total plastics market [1]. The goal of a food packaging material is to protect the food from contamination and oxidation and to extend shelf life of the food. For that reason it is essential that the packaging material works as an oxygen barrier and prevents the gain of moisture [4]. The packaging film must also have good mechanical strength and a certain degree of flexibility [5]. The use of biopolymers, such as polysaccharides, as film barrier materials has received increased interest due to their vast abundance and great oxygen barrier properties [5-7].

The most abundant organic raw material on Earth is wood. Wood is composed primarily of cellulose, hemicelluloses and lignin [8]. Norway spruce (Picea abies) is a predominant softwood species in the North European forest, and are mainly used in the pulp and paper industry [9].The wood hemicelluloses are dissolved in the pulp and paper process but so far there is no retrieval of the polysaccharides which are today seen as a source for the development of new products [10]. The major hemicelluloses in Norwegian spruce are galactoglucomannans and arabinoglucuronoxylans [11-12].

Past research has shown that hemicelluloses have the ability to form plastic like films and coatings. Arabinoxylan from barley husk has been shown to form flexible films without plasticizer. The amorphous films were strong (stress at break 50 MPa) but highly hygroscopic. [13] Glucuronoxylan from hardwood on the other hand needs a plasticizer in order to form films. Gröndahl *et al.* studied the addition of xylitol and sorbitol in different ratios. The films were semicrystalline (44-47 %) and films were stronger (stress at break 40 MPa) and less flexible with less amount of plasticizer. The 35 % (w/w) sorbitol film had and oxygen permeability of 0.21 cm^3 µm m^{-2} d^{-1} kPa^{-1} at 50 % RH. This value is identical to the oxygen permeability of poly(vinyl alcohol) (PVA) film, which is an excellent oxygen barrier material[14-15].

The disadvantage with polysaccharides are their hygroscopic nature which results in a low protection level against water [7, 16]. This can be solved by either laminating the polysaccharide with a water barrier film or chemically modifying the polymer. Gröndahl *et al*. studied the surface gas-phase fluorination of arabinoxylan films. The aim was to make the barley husk arabinoxylan films hydrophobic. The modification resulted in decrease moisture content from 18 to 12 % [17].

Peroval *et al*. [18]investigated cold plasma and electron beam (EB) irradiation to improve the water vapour barrier properties of arabinoxylan films by grafting hydrophobic acrylate monomers onto the surface. The treated arabinoxylan films pre-activated with EB followed by impregnation with additional monomer and a second EB irradiation resulted in a 67 % decrease in water vapour permeability (WVP). Hartman *et al*. [19] developed films with low OP and good mechanical properties from O-acetyl-galactoglucomannan (AcGGM) films. The films were formed by solution-casting from water with the addition of plasticizers such as glycerol, sorbitol and xylitol. The films showed poor results for oxygen permeability. When a binary system of AcGGM and alginate or carboxymethylcellulose (CMC) was used, the mechanical strength and resistance towards humidity increased. The films containing alginate and CMC had an OP of 0.55 and 1.28 cm^3 µm m^{-2} d^{-1} kPa^{-1} respectively at 50 % RH.

2. Aim

The aim of this thesis was to characterize the chemical composition of arabinoglucuronoxylans isolated from Norwegian spruce by mild extraction, study its ability to form films and evaluate the material and mechanical properties of the films from a food package application perspective.

3. Background

3.1. Cell Wall of plants

The plant cell wall is a remarkable structure, it gives the rigidity and shape of plants. The major component of the plant cell wall is cellulose [20]. The first cell wall of the growing cells is called the primary cell wall. When the cell wall stops growing it thickness and new layers are deposited. These new layers are called the secondary cell wall and they are composed of cellulose microfibrils linked by hydrogen bonding to hemicelluloses. This network is embedded in a lignin matrix. A schematic structure of the cell wall is shown in Figure 1.

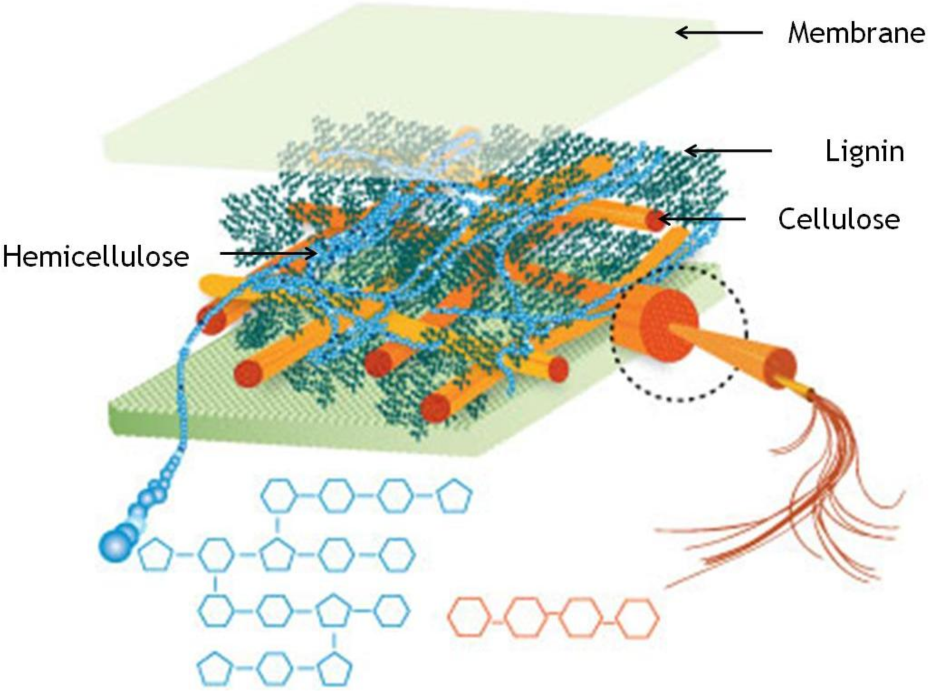

Figure 1 – Plant Cell Wall [21].

Higher plants have larger secondary cell walls enables to become more rigid to support gravitational stresses [22]. The plant cell wall is also composed of different kinds of enzymes, such as hydrolases, and celullases, which cut and cross-link wall polymers.

The quantity of the main components of wood differs if it is softwood or hardwood. Table 1 represents the major structural components of both types of wood.

Table 1 – Contents of main components (% of dry wood) [23].

Type of wood	**Cellulose**	**Hemicellulose**	**Lignin**
Softwood	35-40	25-30	27-30
Hardwood	45-50	20-25	20-25

3.2. Cellulose

The cellulose is the most abundant biopolymer on Earth. Cellulose is an extended linear macromolecule of β-D-glucopyranose units without branches. Structurally, this molecule is a single helix with twofold screw axis [22]. Cellulose composes 20 % of the primary cell wall and 50 % of the secondary cell wall [24]. Cellulose is insoluble in the most of the solvents due to hydrogen bonding. This characteristic is advantageous when separating cellulose from the other constituents of plants. Cellulose is the main constituent of plants, but can also be produced by bacteria (ex. *Acetobacter xylinum*), algae and animal (Tunicin). In spruce wood, cellulose represents approximately 40-50 % [25].

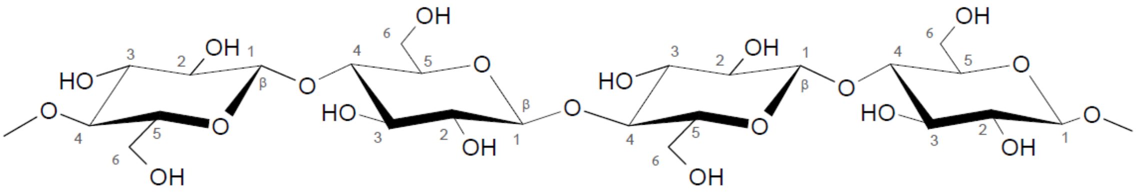

Figure 2 - Structural Unit of Cellulose Molecule.

The translation of every second glucose unit with 180 ° results in a straight and rigid molecule. The absence of side chains allow the molecules to be arranged close to each other. The formation of adjacent chains is possible due to the high amount of –OH groups, each giving an opportunity to make hydrogen bonds. These three properties are perfect to make stiff and elongated fibrils, which is perfect for building the cell walls of plants. The micro fibrils have an average length of 100-40 000 nm and a diameter of 2-20 nm [22]. The thickness, length and degree of polymerization (DP) of cellulose depends on the source and the age of the tissue [24].

According to how it is treated, cellulose is applied to such diverse uses as paper products, anticake agent, emulsifier, stabilizer, dispersing agent, thickener and gelling agent. It is also used in textiles, where the cellulose comes from cotton and linen filaments [20, 26]. Recently, many of the properties of this macromolecule make it an environmentally friendly alternative to oil and gas as a major source of fuel [27].

3.3.Lignin

Lignins are macromolecules composed of phenylpropane units in a complex arrangement. It makes up 20-30 % of wood (w/w). This polymer is an amorphous and the molar mass has been reported to be up to 20 000 g/mol. In wood, the lignin interacts by covalent bonds with polysaccharides, these complexes are called lignin-carbohydrate complexes (LCC). The lignin linkage can be ester or ether type, but the ether linkage is more stable than ester bond. In softwood xylans, lignin can make an ester linkage to a 4-*O*-methylglucuronic acid group or an ether linkage to an arabinose unit (HO-2 or HO-3) [22]. Some lignin-carbohydrate complexes have strong tendency to form micelles or aggregates in aqueous solutions, if they are isolated [28]. In the cell wall, lignin acts as a glue and provides compression strength to the cellulose fibers as well as a hydrophobic surface needed for the transportation of water [29]. It is possible determined total lignin content, and is the addition of Klason Lignin and acid soluble lignin.

3.4.Hemicellulose

Hemicelluloses are the second major components of plant cell walls [30], which are found in the primary and secondary cell walls of land and fresh water plants, and in some seaweed. It’s a group of heterogeneous polysaccharides and is formed by biosynthetic pathways in the Golgi apparatus [31]. The biosynthesis is divided in four steps: chain or backbone initiation, propagation, side chain addition, and termination [32]. After polymerization hemicelluloses are stored in vesicles and later transported out from the cell and integrated with the new synthesized cellulose microfibrils. Their transport within the cell is possible due to their solubility in water. Hemicelluloses are associated with cellulose and are usually a mixture of monosaccharide such as D-xylose, L-arabinose, D-glucose, D-galactose, D-mannose, D-glucuronic acid, 4-O-methyl-D-glucuronic acid and D-galacturonic and to minor amount of L-rhamnose, L-fucose and a variety of O-methylated neutral sugars [22]. These complex polysaccharides are non-crystalline polymers and form hydrogen bonds with cellulose and covalent bonds with lignin. Figure 3 shows some of the most common monosaccharides in hemicelluloses.

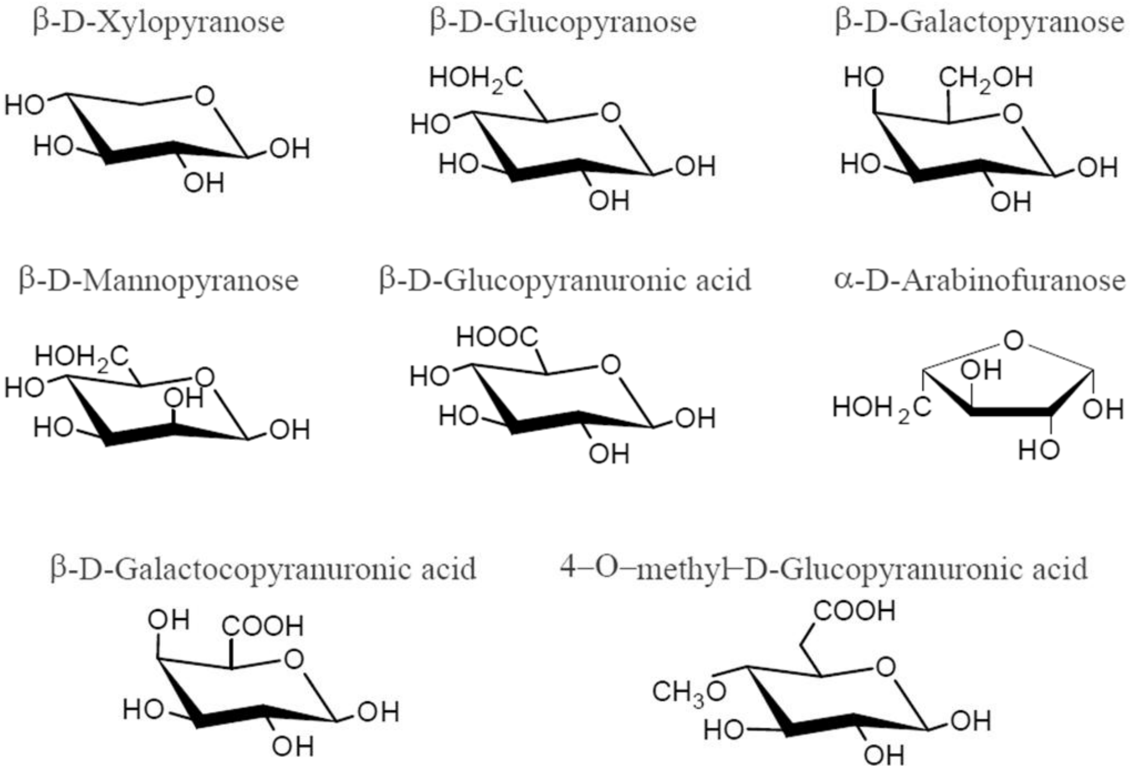
β-D-Xylopyranose β-D-Glucopyranose β-D-Galactopyranose

β-D-Mannopyranose β-D-Glucopyranuronic acid α-D-Arabinofuranose

β-D-Galactocopyranuronic acid 4–O–methyl–D-Glucopyranuronic acid

Figure 3 – The most common monosaccharides in hemicelluloses.

Hemicelluloses differ from cellulose not only in crystallinity aspect but also in DP (about 100 in softwoods and about 200 in hardwoods) and in molar mass, being significantly lower for hemicelluloses. Their general formula is $(C_5H_8O_4)_n$ for a pentosan and $(C_9H_{10}O_5)_n$ for a hexosan [22]. Considerable differences exist in hemicellulose composition and structure between softwood and hardwood. For better understanding, Table 2 summarizes the main compositions of the hemicelluloses in both types.

Table 2 –The major hemicellulose components and their characteristics [22].

Hemicellulose Type	Amount (% of wood)	Composition		
		Units	**Molar ratios**	**Linkage**
Softwood				
Galactoglucomannan	5-8	β-D-Man*p*	3	1→4
		β-D-Glc*p*	1	1→4
		α-D-Gal*p*	1	1→6
		Ac	1	
Glucomannan	10-15	β-D-Man*p*	4	1→4
		β-D-Glc*p*	1	1→4
		α-D-Gal*p*	0.1	1→6
		Ac	1	
Arabinoglucuronoxylan	7-10	β-D-Xyl*p*	10	1→4
		4-O-Me-α-D-Glc*p*A	2	1→2
		α-L-Ara*f*	1.3	1→3
Hardwood				
Glucuronoxylan	15-30	β-D-Xyl*p*	10	1→4 1→2
		4-O-Me-α-D-Glc*p*A	1	
		Ac	7	
Glucomannan	2-5	β-D-Man*p*	1-2	1→4
		β-D-Glc*p*	1	1→4

As can be seen from the above table, hardwood contains mostly xylans, whereas softwood contains mostly galactoglucomannans. For structure details of major softwood and hardwood hemicelluloses see Appendix I. Softwood xylans cannot be directly extracted with alkali as it is necessary to first delignify the cellulose [33]. Some studies on utilization of hemicellulose have demonstrated that they are potentially very useful. One application for hemicellulose is to use them as a fermentation feedstock to produce ethanol, lactic acid, acetone, butanol and xylitol [34]. The hemicelluloses extracted from wheat straw have the ability to serve as adhesives, stabilizers, and also as thickeners and emulsifiers in food [35]. Many studies have demonstrated that hemicelluloses are good film formers [15, 19, 36] and might also have potentials in applications as a nutraceutical [37], in chiral separations [38] and as an HIV inhibitor [39].

3.5. Xylans

Xylans occur in nearly all plants. They are low molar mass heteropolysaccharides (~150 kDa, water soluble solution), and may be branched and/or substituted. Their homopolymeric backbone chain is composed by *β*-D-xylopyranose units with 1,4-linkages. About 80 % of the xylans have arabinose, glucuronic acid or its 4-*O*-methyl ether, and acetyl groups as substituent groups. The occurrence and composition of branches depend on the source of xylan. Hardwood xylans (150-200) have a higher DP compared to that of softwoods (70-130) [40]. The isolation of xylan is often made by alkali treatment, after a necessary prehydrolyzing and delignifying step. Xylans are difficult to dissolve in almost all organic solvents and only partially soluble in aqueous solvents. In industrial scale xylans are used in the production of xylitol, xylose and furfural [41].

3.6. Arabinoglucuronoxylan

The arabino-(4-*O*-methylglucurono)xylans are heteropolysaccharides present in softwoods (5-10%) [22] and are composed of three sugar units: β-D-xylopyranose, 4-O-methyl-α-D-glucopyranosyluronic and α-L-arabinofuranose. Figure 4 is an abbreviated formula with the proportions of the units.

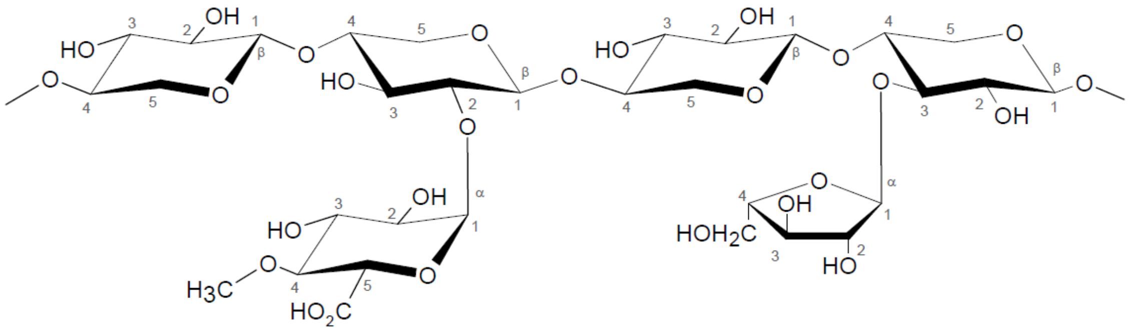

Figure 4 – Principal structure of arabinoglucuronoxylan.

Both the arabinose and uronic acid substituent stabilize the xylan chain against alkali-catalyzed degradation. The average molar ratio of arabinose:methylglucuronic acid:xylose is 1.3:2:10 in softwood xylan [22]. But in spruce heartwood and sapwood this ratio is (2.4-2.5):1.7:10 and the ratio galactose:glucose:mannose is (0.5-0.9):1.1:3 [12]. The arabinoglucuronoxylan is a difficult polysaccharide to isolate in a pure state and in good yields [11].

4. Analytical Methods

4.1. Sugar Analysis

The sugar content in a polysaccharide can be determined by ionic chromatography. Usually a system is composed by a gradient pump, isocratic post column pump, amperometry detector, column oven and auto sampler. The sugar monomers are ionized in strong NaOH (300 mM, 0.5 ml/min) eluent, then separated by anion-exchange chromatography, and finally detected by pulse amperometric detection (PAD) with an electrochemical cell optimized for capillary separations. The method is direct, selective, and sensitive. The carbohydrates from wood samples are separated on a capillary CarboPac PA20 column. The eluents are kept at 4 psi (helium pressure). The internal standard is usually a solution of fucose (400 ppm).

The PAD measures the change in current resulting from carbohydrate oxidation at a gold or platinum electrode. The advantages of PAD are its low detection limits and its suitability for gradient elution. However the detector response decreases with the increase of DP, which is one disadvantage. In one run, HPAED-PAD separate and quantify neutral and acidic monosaccharides. The use of sodium hydroxide as eluent is inexpensive and relatively safe.

4.2. Nuclear Magnetic Resonance

Nuclear Magnetic Resonance, NMR, is an excellent physicochemical technique for determining the structure of polysaccharides. Also it can be used to identify monosaccharide composition, elucidate linkage patterns, glycosidic configurations and establish the sequence of sugar units.

The operating principle of NMR is based on the absorption and remittance of electromagnetic energy when a magnetic nucleus is affected by a magnetic field. This energy is at a specific resonance frequency which among others is dependent on the magnetic strength. All isotopes with an odd number of protons and/or neutrons have an intrinsic magnetic moment and angular momentum a so called non zero spin. Radio frequency radiation of appropriate energy is subjected to the sample of interest. The frequency is either varied and the magnetic field set constant or the magnetic field is varied or sweeped over the sample. When the pulsed radio frequency is removed, the energy is released; this simultaneously results in a signal. The signal represents the structural information about the individual nucleus and its surroundings. The signal is detected, analyzed and expressed, in ppm, as a chemical shift, δ. The most common NMR proton (^{1}H) and carbon (^{13}C).

All chemical shifts of carbohydrates in ^{1}H NMR spectroscopy are in the range of 1 to 6 ppm, where most of the α-anomeric protons appear in the region of 5 to 6 ppm and most of the β-anomeric protons appear in the 4 to 5 ppm. The proton signals are more sensitive compared to ^{13}C signals due to their natural abundance. However, most of the proton signals appear in the region of 3 to 5 ppm, which results in an overlap of signals indistinct. One solution is to use two or multi-dimensional NMR techniques, that improves the resolution and sensitivity of the signals.

One advantage when using ^{13}C NMR is the absence of overlap of signal, because in this case the chemical shifts spread at a large range. In ^{13}C NMR spectrum, signals from the nonanomeric carbons appear between 60 to 85 ppm, α-anomeric protons are in the region of 95 to 103 ppm and β-anomeric protons are in the 101 to 105 ppm. To study a NMR spectrum, ^{1}H and ^{13}C, of an unknown polysaccharide, it’s first necessary to compare the spectrum with literature values. To do a full analysis of the structure one needs to complete a 2D NMR [42].

4.3. Size Exclusion Chromatography

Size exclusion chromatography (SEC) is an important test method for the determination of the average molar mass of macromolecules. The molecules are separated according to their size e.g. hydrodynamic volume in solution using a column. The material is dissolved in a proper eluent and the solution is injected onto a column consisting of a porous matrix e.g. polyacrylamide, crosslinked polystyrene or silica. The separation of the molecules is due to size. Larger molecules are eluted first while small molecules elute late as they are travelling through the pores within the stationary phase. The solute is either collected in fractions or constantly monitored. To determine the concentration of molecules a spectroscopic technique is often used e.g. refractive index (RI) or ultraviolet (UV) light. From a standard curve of known molar mass it is possible to determine the average molar mass of the solute in reference to the standard material. This is not the true molar mass of the sample as an assumption is made that the molecule of interest has the same hydrodynamic ratio as the standard material. In order to get the true molar mass a light scattering detector is needed.

The amount of light scattered (LS) is directly proportional to the product of the weight average molecular weight and the solute concentration, i.e. LS~M_w*c [43]. A mathematical formula based on Zimm and Debye describing this relation has been derived:

$$\frac{Kc}{R_\theta}=\frac{1}{M_w P(\theta)}+2A_2c \tag{4.1}$$

where: K is the optical parameter, which is constant

c is the sample concentration

R_θ is the intensity of light scattering at the angle θ

M_w is the weight average molecular weight

$P(\theta)$ is a function that describes the angular dependence of scattered light

A_2 is the second osmotic virial coefficient

The optical constant can be expressed as the next equation:

$$K=\left(\frac{4\pi^2 n_0}{\lambda_0 N_A}\right)\left(\frac{dn}{dc}\right)^2 \tag{4.2}$$

where: n_0 is the refractive index of the solvent

λ_0 is the wavelength of the incident light

N_A is the Avogadro's number

The dn/dc value, the change of solution refractive index with respect to a change in concentration of the molecular species being measured, can be determined at room temperature using a refractometer. By recording the electric potential difference (ΔV) for each concentrations the refractive index can be calculated according to,

$$\Delta n=\Delta V\left(\frac{d(n)}{d(v)}\right) \tag{4.3}$$

where $\frac{d(n)}{d(v)}$ is the RI constant for the calibrated refractometer used.

The specific refractive increment can be calculated from the slope by plotting the refractive index for each concentration as a function of the concentration of the solute according the relation:

$$\Delta n = \Delta c \frac{\mathrm{d(n)}}{\mathrm{d(c)}} \tag{4.4}$$

At the end of the analysis it is obtained a molecular size distribution curve, and average molar mass is calculated using Astra software. The software calculates the molar mass for each angle and produce a Debye plot, where $\mathrm{Kc}/\mathrm{R}_\theta$ is function of $\sin^2(\theta/2)$. The intercept gives the average molar mass $1/\mathrm{M_W}$.

The relative molar mass can also be determinate using Pullulan standards. Pullulan is a linear polysaccharide consisting of three glucose molecules, which are linked with α-1,4 glycosidic bonds. Each Pullulan standard corresponds to an average elution volume. A standard curve is plotted where the molar mass is a function of average elution volume. The elution volume of the sample is known and the relative molar mass can be determined from the standard curve.

4.4. Wide Angle X-ray Scattering

Wide Angle X-ray Scattering (WAXS) is a technique that can be used to determine the degree of crystallinity of a material. The sample is scanned in a wide angle X-ray goniometer, and the final result is a plot where the scattering intensity is read as a function of the 2θ angle. The reading is usually carried out using oriented fibers or films [42].

Constructive X-ray diffraction will only take place if the path of the difference between the rays is equivalent to an integral number of wavelength. If the spacing between atomic planes are defined d_{hkl}, θ is the angle that those atomic planes make with the incoming X-ray beam, λ is the wavelength of the X-ray beam (1.5418 Å for CuK_α) and n is an integer which defines the order of diffraction.

The spacing between adjacent reflection planes and diffraction angle are related according to Bragg's law:

$$\frac{2\sin\theta}{\lambda} = \frac{n}{d_{hkl}}, \quad n = 1,2,3,\ldots \tag{4.5}$$

The observed reflections are indexed in terms of Miller indices (h,k,l) for each crystallographic plane. Then, they are used to determine the lattice constants a, b and c. The lattice parameter/restrictions defined seven crystal systems: cubic, tetragonal, orthorhombic, monoclinic, triclinic, hexagonal and trigonal.

These two parameters are related according the next equation in orthorhombic unit cell case:

$$\frac{1}{d_{hkl}^2} = \frac{h^2}{a^2} + \frac{k^2}{b^2} + \frac{l^2}{c^2} \tag{4.6}$$

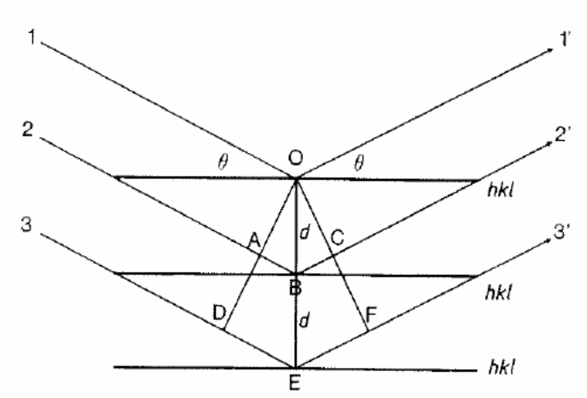

Figure 5 - Diffraction of x-rays at a set of lattice planes in a crystalline substance [44].

The X-ray source and the detector lie on the so-called goniometer circle at which centre the polymer sample is placed. During running the polymer sample is turned at an angular velocity ω whilst the detector turns around the sample at an angular velocity of 2ω. As long as the anticathode is stationary, the sample will be in focus and a Bragg reflection can be obtained for every angle θ. The intensity is usually plotted as a function of twice the angle, 2θ.

Each sample has a unique X-ray diffraction pattern due to number of peaks, the positions of the peaks and the intensities of the peaks [45].

The degree of crystallinity, X_C, can be calculated by integrating the intensity of the crystal diffraction peaks (A_C) and divide by the integrated intensity for the amorphous diffraction (A_A).

$$X_C = A_C/(A_A + A_C) \tag{4.7}$$

4.5.Tensile Testing

Tensile testing is used to analyze the mechanical behavior of a material by subject a material to unaxial tension until failure. The equipment register the force needed until the material breaks. From the tensile profile, stress-strain curve, the stress at break, yield point and the fracture point can be distinguished, see Figure 6.

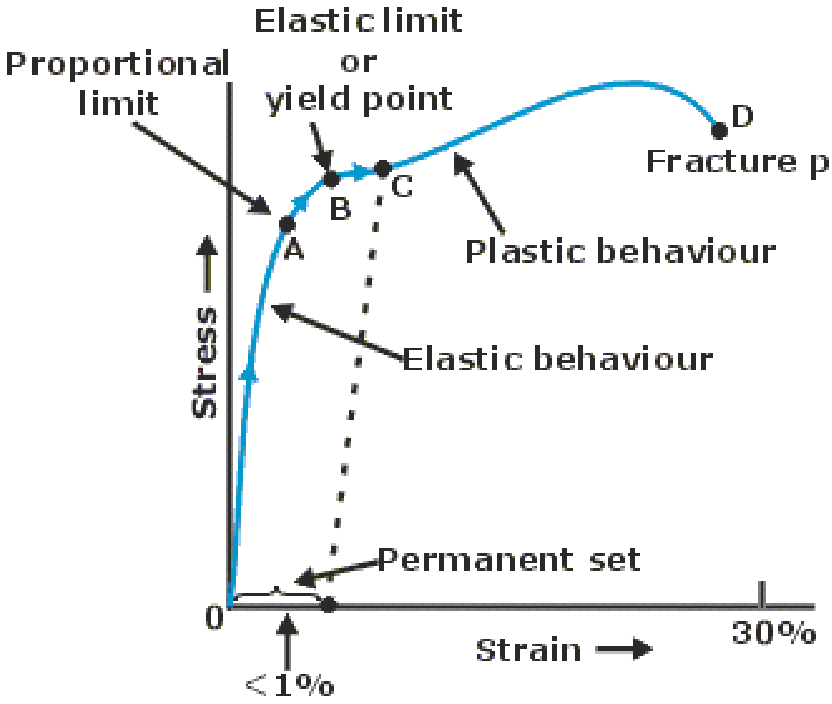

Figure 6 – Typical Stress-strain diagram [46] .

The stress is the average force per unit area and is defined as,

$$\Sigma = \mathrm{F}/\mathrm{A} \tag{4.8}$$

where F is the force applied and A the cross section area. The elongation of the sample, strain is defined as,

$$\varepsilon = \frac{\Delta L}{L} \tag{4.9}$$

where ΔL is the increment of length caused by the force applied and L is the initial length. In the initial portion of the tensile profile the applied force and the elongation are in linear relationship between. The relationship is defined as Hooke's Law,

$$E = \frac{\sigma}{\epsilon} \tag{4.10}$$

where E is the Young's Modulus.

Depending on sample material e.g. thin films, plastics, rubber different test methods are used and different test specimen needed e.g. strips or dogbones.

4.6.Dynamic Mechanical Analysis

Classical materials exhibit either elastic or viscous behavior in response to an applied stress. In solid materials, elastic responses are typical, i.e., when a stress is applied to an elastic system it deforms proportionally by a quantity identified as the strain. In viscous behavior, which is a characteristic of fluids, the bond energies necessary for long range translational order have been overcome. An applied stress results in a strain that increases with time until the stress is removed. Viscoelastic behavior of a polymer means that the material has both solid and liquid characteristics that change with temperature, time or frequency. In a viscoelastic system the stress decreases with time. Since modulus is defined as the ratio of stress to strain, it can be seen that the modulus calculation in viscoelastic system must incorporate a time function and cannot be considered as an immutable property independent of the period over which the measurement is made.

Dynamic Mechanical Analysis, DMA, measures the modulus (stiffness) and the damping (energy dissipation) properties as a material deforms under periodic stress. It can be operated in a controlled stress or controlled strain mode. In the dynamic experiment, i.e., in a controlled stress mode, the equipment applies an oscillatory stress with a controlled frequency. The response using this method is a function of frequency rather than time and the stress function is sinusoidal. For a perfect elastic material the applied stress and the resulting strain will be in phase (as illustrated in Figure 7 a)) but for a viscous behavior the stress will lead the strain by 90 ° (as shown in Figure 7 b)).

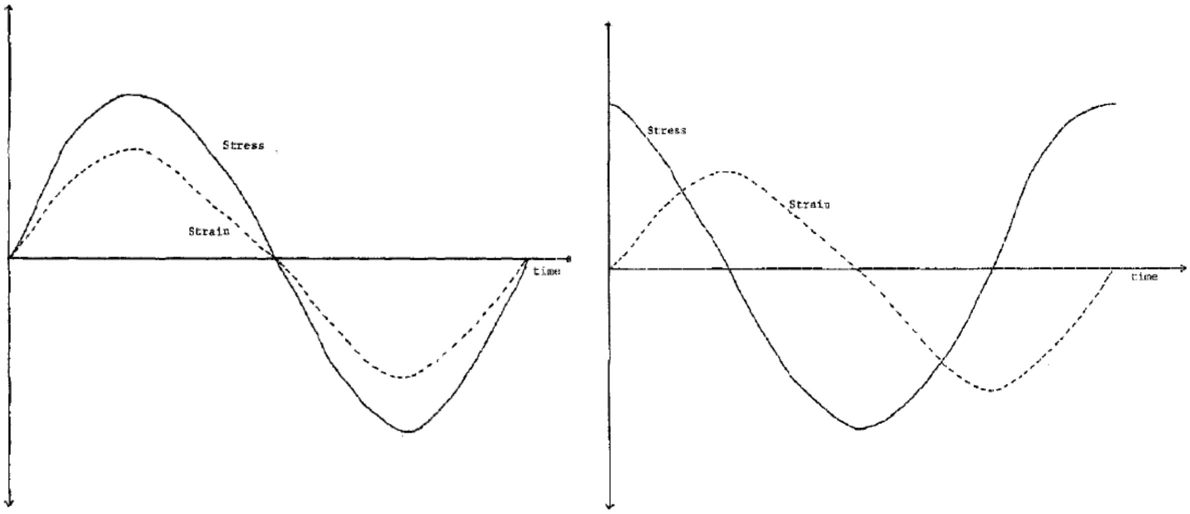

Figure 7 – The behavior of two systems under oscillatory stress: a) elastic b) viscous[47].

A viscoelastic material will give some hybrid of these two responses. The stress and strain will be out of phase by some quantity know as the phase angle and commonly referred as delta (δ). The stress and strain functions are shown below:

$$\text{Stress:} \qquad \sigma(t) = \sigma_0(t)\sin(\omega t + \delta) \tag{4.11}$$

$$\text{Strain:} \qquad \varepsilon(t) = \varepsilon_0(t)\sin(\omega t) \tag{4.12}$$

where: ω is the angular frequency

t is the time

The existence of the stress in two components (lagged) suggests its representation in the complex plane. Thus complex representations of the stress and strain are related:

$$\sigma^*(t) = \sigma_0 e^{i(wt+\delta)} \tag{4.13}$$

$$\varepsilon^*(t) = \varepsilon_0 e^{i(wt)} \tag{4.14}$$

Where it is possible define a complex modulus,

$$E^* = \frac{\sigma^*(t)}{\varepsilon^*(t)} = \frac{\sigma_0}{\varepsilon_0} e^{i\delta} = E' + iE'' \tag{4.15}$$

The storage modulus and the loss modulus are defined as follows:

$$\text{Storage modulus:} \qquad E^{'} = E^{*}cos(\delta) \tag{4.16}$$

$$\text{Loss modulus:} \qquad E^{''} = E^{*}sin(\delta) \tag{4.17}$$

The complex response of the material is resolved into the elastic or storage modulus (E’) and the viscous or loss modulus (E’’) if the deformation is in the shear mode. The storage modulus, called elastic modulus, is a measure of a sample’s ability to store energy and is related to the stiffness of the material and the loss modulus is a measure of a sample's ability to dissipate energy as a result of molecular motions and reflects the damping characteristics of the material. The ratio of the loss modulus to the storage modulus is called tan δ, and represents the damping properties of the sample.

$$E''/E^{'} = Tan(\delta) \tag{4.18}$$

DMA is normally used to study the thermal transitions of a material by studying the changes in modulus as a function of temperature. Loss modulus and storage modulus can also be studied as a function of humidity, where the temperature, frequency and amplitude of the induced strain is set constant.

4.7. Water Vapour Sorption

Water Vapour Sorption (WVS) is a valued tool to understand the surface adsorption effects of water and organic vapours. This method enables the prediction if a material will gain or lose water when exposed to a particular humidity condition. This property is accepted as an important factor to determine the storage, stability, processing and application performance of a film [48]. The sample is subjected to varying conditions of humidity and temperature, and the response of the sample is measured gravimetrically. In isotherm experiments, a weighed sample is “dried” and exposed to different humidities changed at a fixed temperature. The sample is kept at each humidity level until no further weight change is detected. Data points with relative humidity and moisture gain is recorded and the process repeated in an increasing or decreasing procedure [49]. Figure 9 shows a typical water sorption result from a WVS experiment.

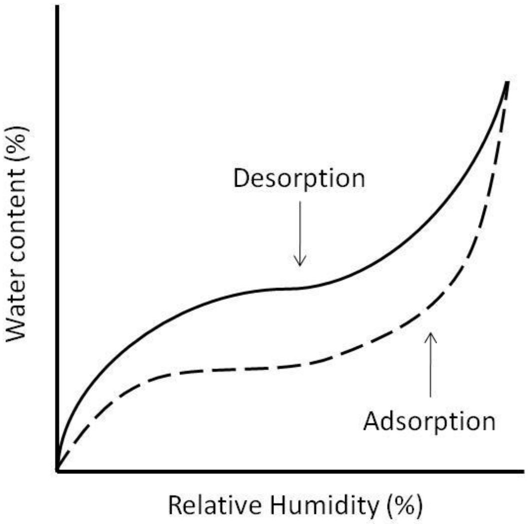

Figure 8 – General water sorption isotherm showing a hysteresis.

For the same relative humidity the amount of water in adsorption and desorption may differ, which is called hysteresis. This phenomenon is shown in Figure 9. There are two possible reasons for hysteresis to exist. Firstly, condensate of water in capillaries may evaporate differently during the drying step. Finally, hysteresis are based on phase changes of non-porous solids or structural changes of non rigid solids resulting in binding of more water [50-51].

4.8. Oxygen Permeability

The oxygen permeability (OP) measures the ability of oxygen to diffuse through a film. The film is placed in a diffusion cell and oxygen-free carrier gas is used to clean the cell from oxygen, and then pure oxygen is introduced to the outside chamber of the diffusion cell. The oxygen diffuses through the film and then reaches the oxygen sensor, which generates a signal that is proportional to the amount of oxygen in the carrier gas. The measuring is complete when the concentration of oxygen in the carrier gas side atmosphere is constant. In agreement with ASTM D3985 the carrier gas is nitrogen. Figure 10 is an example of a test chamber for an oxygen permeability test.

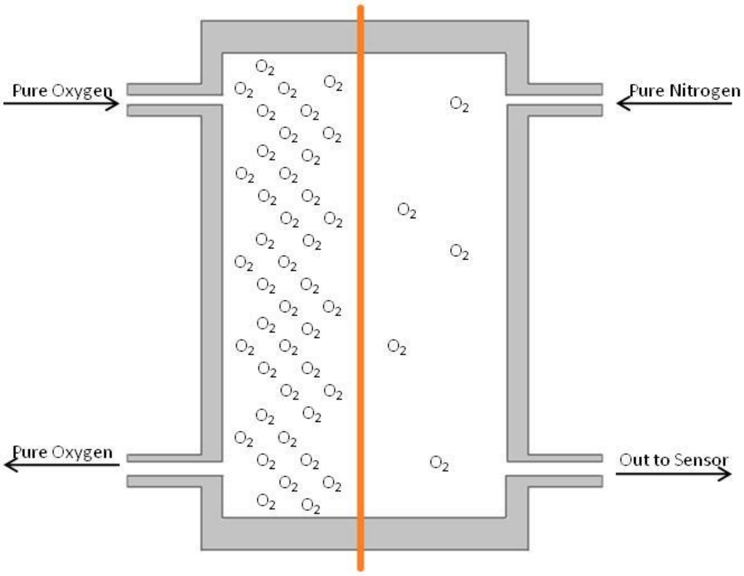

Figure 9 – Oxygen Permeability Test.

The final result is expressed as the oxygen permeability coefficient (OPC), but sometimes the result is expressed as the oxygen transmission rate (OTR). The OPC is calculated according to the formula:

$$\mathrm{OPC} = \frac{\mathrm{l} \times \Delta \mathrm{m_{gas}}}{\Delta \mathrm{t} \times \mathrm{A} \times \Delta \mathrm{P}} \qquad (4.16)$$

Where: Δm_{gas} is the quantity of permeant (cm^3)

l is the thickness of polymeric barrier (µm)

Δt is the duration of permeance (day)

A is the area of barrier (m^2)

ΔP is the partial pressure difference across the barrier (kPa)

The OTR is usually reported in cubic centimeters of gas that pass through a square meter of film in 24h when the partial pressure difference is one atmosphere. The correlation between the OTR and OPC is expressed by the equation:

$$\mathrm{OTR} = \frac{\mathrm{OPC} \times 1\mathrm{atm}}{\mathrm{l}} \qquad (4.17)$$

5. Experimental

5.1. Materials

The arabinoglucuronoxylan (AGX) portion was obtained from Norway Spruce by alkali extraction using Wise and Timell methods [52-53].

5.2. Preparation of Films

Films were prepared by mixing AGX, pure or mixed with plasticizer, with deionized water under magnetic stirring at 70 ºC for 15 minutes. The total amount of dry substance in each film was kept constant at 2.5 % (w/w). The solutions were poured onto polystyrene petri dishes. The films were dried at 25 ºC and a relative humidity (RH) of 30, 50 and 70 %. No difference in either crystallinity or mechanical properties were seen as an effect of different humidity when film was formed which is why 50 % RH was used thereafter. The formed films were conditioned at 50 % RH before characterization.

5.3. Composition Analysis

The sugar content was determined by an ICS-3000 Dionex (Dionex, Sweden). The system was equipped with a gradient pump, column oven, autosampler and one guard column followed by AEC column capable of separating monosaccharide's (ProPac Pa 4x250 mm, CarboPac PA 1 4x250 mm). AGX was hydrolyzed by 72 % hydrochloric acid (200 mg AGX, 3 ml of H2SO4) [54]. The AGX solution was first impregnated under vacuum for 15min followed by heating in a water bath (30 ºC) for one hour. Deionized water (84 ml) was added and the sample was autoclaved at 125 ºC for 1 hour. The material was filtered through a PVDF filter (GV, Millipore, 0.22 µm). The filtrate was collected and the volume was adjusted to 100 ml with deionized water. 5ml of the sample was added to a volumetric flask (50 ml) along with 5ml fucose (400 mg/l) as an internal standard. The volume was adjusted with deionized water. The sample was filtered again into 1.5 ml vials (GHP, PALL, 0.45 µm).The arabinose to xylose ratio was calculated by relating the area of the recorded peaks. The Klason Lignin was also determined gravimetrically as the insoluble material after hydrolysis according to the Uppsala method [55].

5.4.Nuclear Magnetic Resonance

The ^1H and ^{13}C NMR spectra were recorded on a Bruker Avance III 600 MHz spectrometer using a 5.0 mm $^1H/^{13}C/^{15}N/^{31}P$ inverse detection QXI probe, equipped with z-gradients and controlled by Topspin 2.1 software. The NMR spectra were obtained for ^2H_2O solution of ca. 20 mg polysaccharide at 25 ºC using acetone (δ_H 2.225, δ_C 31.05) as internal reference. The data were acquired and processed using Bruker Topspin software. The signals were assigned using 1D and 2D experiments, TOCSY, NOESY, HSQC, HSQC-TOCSY and HMBC from the Bruker library. The relaxation delay between successive pulse cycles was 1.5 s for COSY and TOCSY and 2 s for NOESY. The TOCSY experiments were carried out with mixing times of 30 and 90 ms, NOESY with 100 and 300 ms, HSQC-TOCSY experiment with 80 ms, and HMBC with 60 ms.

5.5.Size Exclusion Chromatography

The molar mass of the arabinoglucuronoxylan was determined using a HPSEC-MALS-RI-UV aqueous system of Waters 2690 (Waters Corporation, Milford, MA, USA). The system had an online degasser; auto sampler; column oven and three serial connected columns (Shodex OHpak SB-803 HQ, SB-804 HQ and SB-806M HQ) controlled at 50 °C. The detectors were multi-angle laser light scattering (Dawn DSP equipped with a He-Ne laser at 632.8 nm, Wyatt Technology corp., Santa Barbara, CA, USA); refractive index (RI) controlled at 35 ºC (Optilab DSP, Wyatt Technology corp.) and a UV-VIS detector set to record at 280 nm (Shimadzu SPD-10A, Shimadzu corp., Kyoto, Japan). The eluent used was sodium nitrate (0.1 M $NaNO_3$) containing 0.02 % sodium azide (NaN_3). The flow rate was 0.4 ml/min. All samples were dissolved in 0.1 M $NaNO_3$ solution at a concentration of 2 % (w/w) and filtered

(GHP syringe filter, 0.45 µm, PALL). The range of angles available for determination was 30–150 °. The dn/dc used was 0.146ml/g [56]. The weight-average molar mass was determined using ASTRA3 software. The SEC was also run in a strongly alkaline sodium hydroxide/acetate solution (0.2M hydroxide and 0.1M acetate, pH 13) according to previously described method [57].

5.6. Wide Angle X-ray Scattering

The crystallinity of the xylan films was determined using a Siemens D5000 goniometric diffractometer (Munich, Germany). The film was placed in the diffractometer in one layer. Diffractograms were recorded in the reflection geometry using CuK$_\alpha$ radiation with a wavelength of 1.54 Å. Diffractograms were taken between 5 ° and 50 ° (2θ) at a rate of 1 ° (2θ) per minute, a step size of 0.1 (2θ) and the divergence split fixed to 0.5 mm.

5.7. Tensile Testing

The mechanical properties of the conditioned arabinoglucuronoxylan films were determined by a tensile testing machine (Lloyd L2000R) with a load cell of 100 N. The method used was pull to break. The test took place at room temperature (25 ºC) at a fixed humidity (50 % RH). The samples were cut into strips 9.4 mm in width using a punch. The thickness of the samples was determined by a micrometer (Mitutoyo, Japan). The gauge length was set to 35 mm, speed at 5 mm/min and preload at 0.5 N. For each sample, five replicas were made. The stress and strain at break was recorded and the Young’s modulus calculated using Nexygen MT software (Ametek, FL, USA).

5.8. Dynamic Mechanical Analysis

DMA was used to measure the storage modulus (E’) and loss modulus (E’’). Humidity scan was used to analyze the softening of the arabinoglucuronoxylan films. The scan was performed in a DMA Q800 (TA instruments, New Castle, DE, USA), which had an extension connected to a humidity controller. The films were cut into strips (9.4x10 mm). The samples were loaded at 1 Hz frequency, 125 % force track and amplitude at 5 µm. The temperature was fixed at 25 ºC and the humidity ramp was 1 % RH per 10 minutes starting at 0 % up to 90 % RH.

5.9. Water Vapour Sorption

The arabinoglucuronoxylan films were conditioned in a constant temperature and humidity controlled chamber. The temperature was set to 25 ºC and the relative humidity was changed between 10 to 90 %. The equilibrium water content was measured gravimetrically in a balance and calculated as the weight of water in the sample compared to the total weight. The change in weight was plotted and illustrated as the water vapour sorption isotherm.

5.10. Oxygen Permeability

The oxygen transmission rate was measured using an 8001 Oxygen Permeation Analyzer (Systech Instruments, UK) in accordance with ASTM D3985-81. Duplicate samples with the sample area 5 cm^2 were analyzed at the same time in two separate cells. Nitrogen flowed through the cells for 40 minutes to clear the chamber from oxygen. The analysis was made in 50% RH after conditioning of the samples. The temperature and relative humidity of the test conditions were 25 ºC and 50% RH respectively. The data were recorded when the OTR level was stable. The thickness of samples was measured with 5 replicates, and the OPC was calculated with the partial pressure difference of 101.3 kPa.

6. Results and discussion

6.1. Characterization

6.1.1. Sugar Composition

The sugar composition of the Spruce xylan was measured by Dionex. The results are shown in Table 3. The sample consisted essentially of the monosaccharides xylose, arabinose and 4-*O*-methyl-glucuronic acid.

Table 3 – Sugar content (% w/w) of arabinoglucuronoxylan sample.

Xyl	Ara	Glc	Gal
87.55	8.06	3.04	1.35

The results give an arabinose to xylose ratio of 9.21±0.02 % and the Klason Lignin was 16±1 %. A typical chromatogram from the sample analysis is shown in Figure 11.

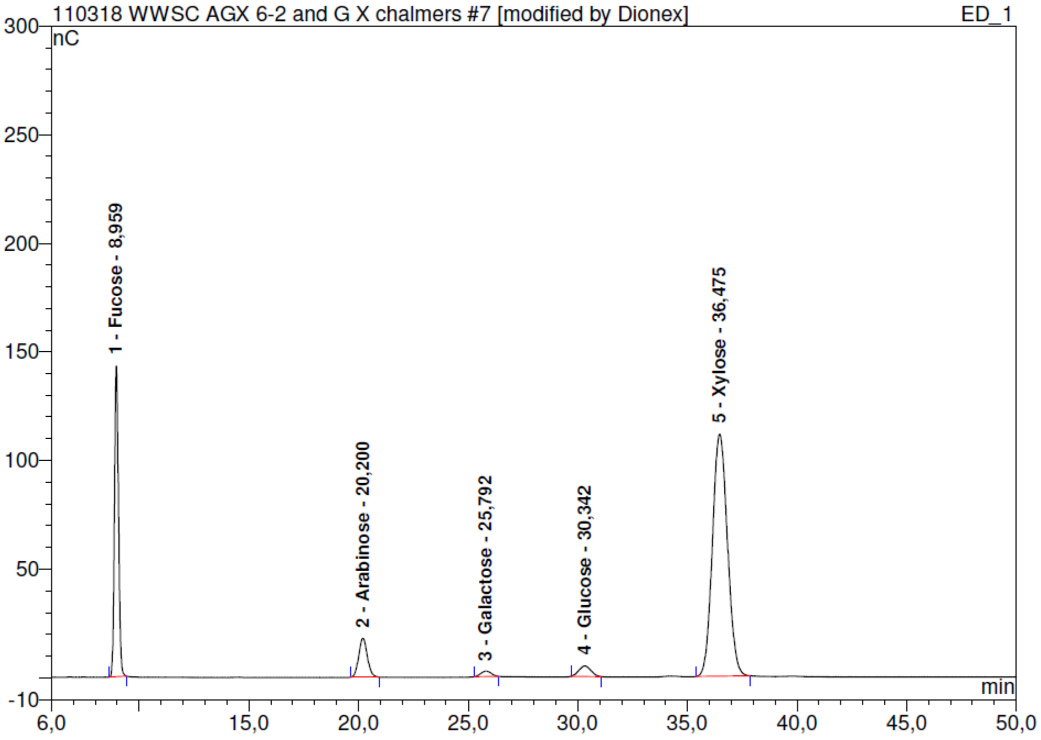

Figure 10 – Chromatogram from Dionex Analysis.

The chromatogram shows a good separation between the peaks. In this method the 4-O-methyl glucuronic acid wasn’t detected because this side group was converted to hexenuronic acid during the acid hydrolysis.

Due to this problem, the sample was sent for an external analysis to Innventia AB (Sweden). The method used was capillary electrophoresis (CE) but also enzymatic degradation as pretreatment the according to O.Dahlman *et al.*, 2000, J.Chromatogr. A, 891 (1), 157-174. The result is summarized in Table 4, and in this analysis the arabinose-xylose ratio was 8.57 %.

Table 4 – Sugar composition (% w/w) with CE analysis.

Xyl	**4OMeGlcA**	**Ara**	**Glc**	**Others sugars**
80.5	10.0	6.9	2.0	0.6

When comparing the two different analyses show good agreement with one another. The spruce xylan contained xylose and was as much as 17% substituted with arabinose and 4-O-methyl glucuronic.

6.1.2. Structure Determination

The arabinoglucuronoxylan was studied by NMR spectroscopy to determine the primary structure, the ^{1}H NMR spectrum is shown in Figure 12. Two signals were observed in the α-anomeric proton region between 5.2 and 5.4 ppm, and they indicate that the minor structural elements in the sample were α-L-arabinofuranose (5.384) and α-D-glucopyranuronic acid (5.271). In the β-anomeric proton region, between 4.4 and 4.7, it’s possible to observe five signals, which show that the major structural elements in the sample is β-D-xylopyranosyl. The ratio arabinose:glucuronic acid:xylose was 1:2:11 and it was determined by integration of anomeric protons. Comparing the NMR results and the Dionex results, the glucuronic acid content was lower (4.3 %) in the first method.

After the analysis of 1D, 2D, TOCSY, NOESY, HSQC, HSQC-TOCSY, HMBC experiments, it is not possible to say if the substituent groups on the main xylose chain were random or in blocks.

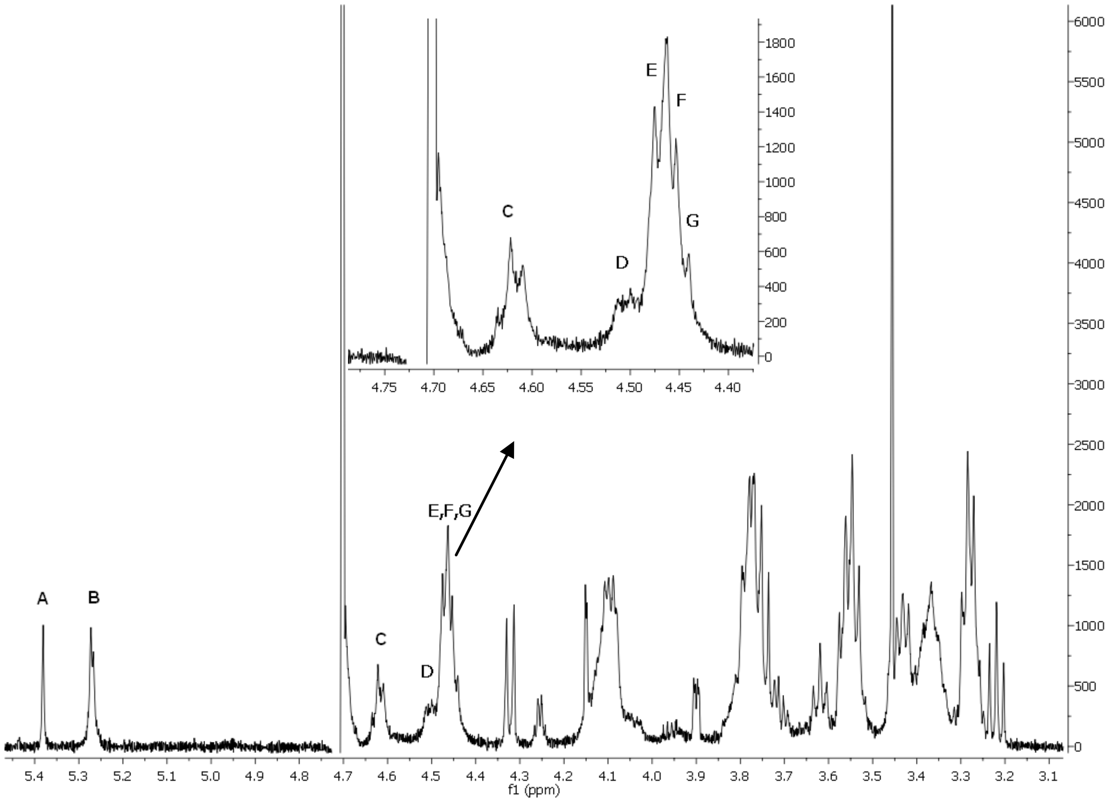

Figure 11 – 1H NMR spectrum of arabinoglucuronoxylan from spruce (D_2O, 27ºC).

However, the observation of NOESY from the anomeric protons atoms shows that there is at least one free xylose (E) between two substitutions. Table 5 shows the results of NOESY and Figure 13 shows the main chain with side chains.

Table 5 – Selected inter-residue NOESY from the anomeric protons atoms.

Residue		**H-1** **δ$_H$ (ppm)**	**Connectivities to:** **δ(ppm)**	**Inter-residue** **atom/residue**
α-L-Ara*f*-(1→3)	**A**	5.384	3.743 (s)	H3 of D
			4.505 (m)	H1 of D
			4.447 (w)	H1 of G
4-*O*Me-a-D-Glc*p*A-(1→2)	**B**	5.271	3.428 (s)	H2 of C
			4.614 (m)	H1 of C
			4.458 (w)	H1 of F

(s) strong NOE, (m) medium NOE, (w) weak NOE

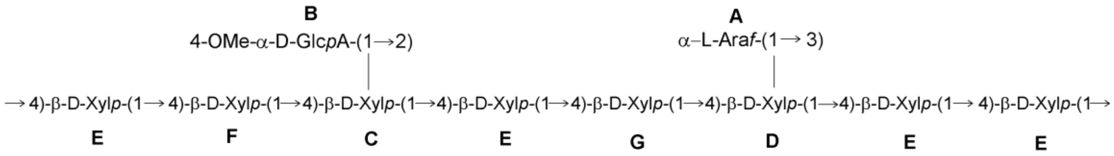

Figure 12 – The distribution of side chains on the main xylose chain.

6.1.3. Molar mass

The molar mass of arabinoglucuronoxylan was analyzed using SEC. Figure 14 shows the refractive index signal, which illustrate the concentration profile of the sample, and the light scattering signal for the sample illustrating the molecular distribution related to size.

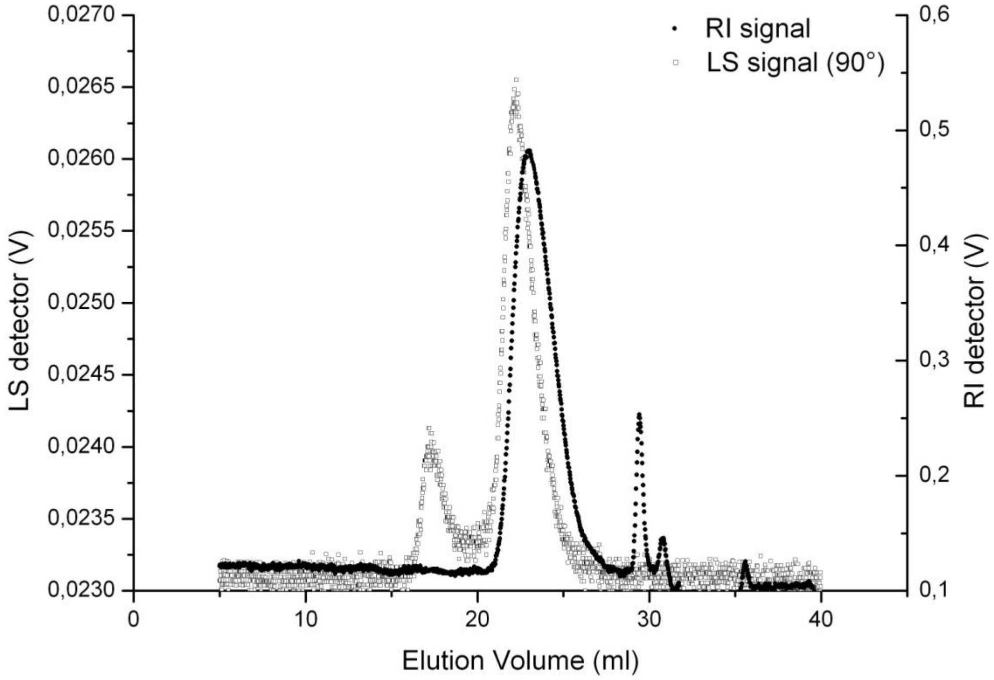

Figure 13 – Molar mass distributions of sample and LS signal.

The light scattering (LS) signal showed two peaks. The peak between 20 and 25 ml represented the molecularly dissolved xylan and the peak at 15 and 20 ml most likely aggregated xylan. It is clear from the chromatogram that the first peak is low concentration as it is not giving rise to any RI signal. The RI signal for the second peak is slightly-shifted towards the lower portion of molecular distribution. The average molar mass (M_w) was 12 780 ± 65 g/mol.

The dn/dc of arabinoglucuronoxylan was also determined in off-line mode and the value obtained was 0,0637 ml/g. The average molar mass obtained was 53 230 ± 267 g/mol. Although the dn/dc value was determined correctly, the concentration interval of the refractometer cell was not in range of literature dn/dc, which probably underestimated the dn/dc and thereby overestimated the molar mass.

The relative molar mass was also determined using Pullulan standards. The relative molar mass obtained was 42 140 g/mol. The standard is probably not adequate for arabinoglucuronoxylan due to the fact that they have different tacticities. The Pullulan is syndiotactic polymer, which means that it has a linear configuration. Arabinoglucuronoxylan is an atactic polymer because the substituent groups are placed randomly along the chain. Structurally arabinoglucuronoxylan has a random configuration. Due to their random nature atactic polymers are usually amorphous.

6.1.4. Film formation

Films were cast from water solution with and without addition of sorbitol as plasticizer. All samples gave homogeneous and transparent films, which were easy to handle and were of similar thickness (50 µm), regardless of the plasticizer level. Figure 15 shows an example of arabinoglucuronoxylan film prepared in this work.

Figure 14 – Film from water casting.

6.1.5. Morphology

The morphology of the arabinoglucuronoxylans films was studied using WAXS. Figure 16 shows the diffractograms of spruce xylan films, with or without sorbitol as plasticizer.

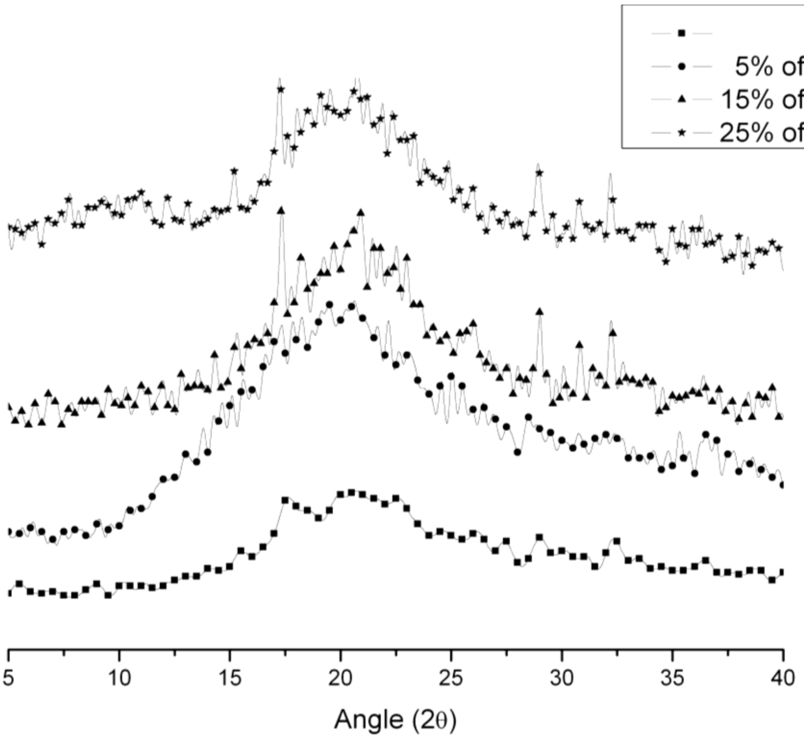

Figure 15 – X-ray diffractograms of Arabinoglucuronoxylan film and plasticized films.

The pure arabinoglucuronoxylan film was completely amorphous. Small peaks of crystallinity could be seen in the 15 and 25% plasticized films. This indicated crystallization of sorbitol in distinct phases. The spruce xylan films were transparent due to the absence of crystallinity.

Different humidity conditions, 30% and 70%, were evaluated when casting xylan films. From X-ray it could be concluded that the films were amorphous and relative humidity therefore does not seem to play a role in crystallization in film formation. For the analysis of these diffractograms see Appendix 2.

6.2.Mechanical Properties

6.2.1. Tensile Testing

The mechanical properties were evaluated by tensile testing at 50% RH, typical stress-strain curve for the arabinoglucuronoxylan films with and without plasticizers, are shown in Figure 17.

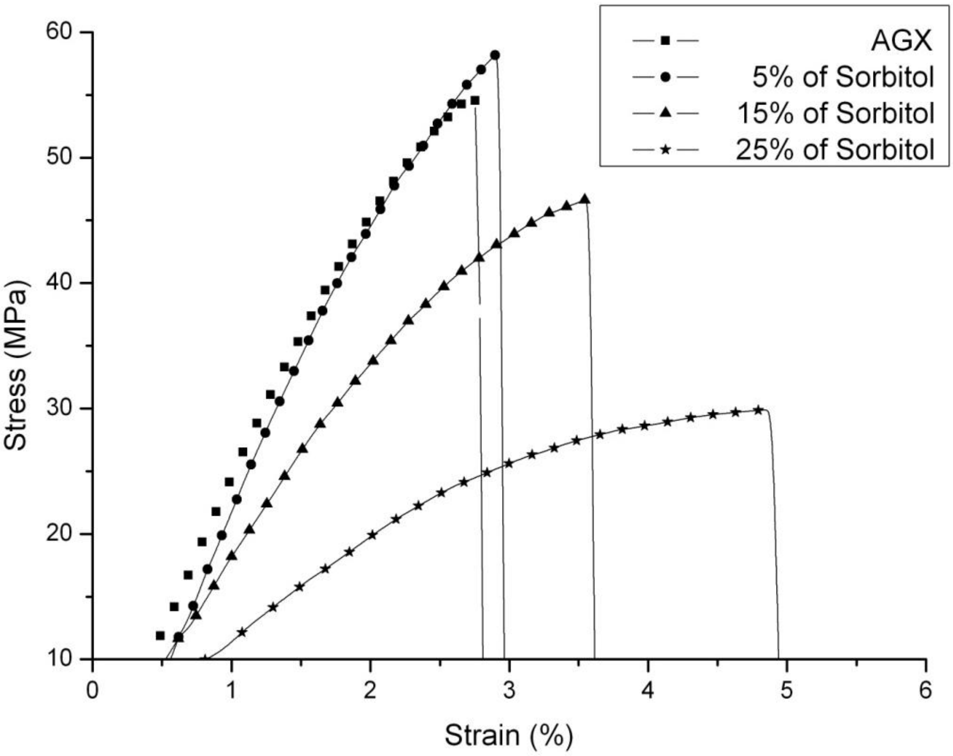

Figure 16 – Stress-Strain curves of sorbitol plasticized films.

In general, the arabinoglucuronoxylan films presented a decrease in tensile stress with higher plasticizer contents. In contrast, sorbitol films with 5, 15 and 25% of sorbitol were more flexible than the non plasticized film, i.e., values in elongation at break were higher.

Arabinoglucuronoxylan film were strong with a stress at break above 55 MPa, but quite flexible, with a strain at break around 2.7 %. The Young's Modulus was 2 735 MPa. Table 6 summarizes the results of tensile tests.

Table 6 - Results of stress-strain curve.

Sample	**Young's Modulus (MPa)**	**Stress at break (MPa)**	**Strain at break (%)**
Control	2735 ± 388	55 ± 7	2.7 ± 0.7
5%	2612 ± 160	57 ± 1	3.1 ± 0.3
15%	2063 ± 109	44 ± 2	3.3 ± 0.8
25%	1163 ± 140	26 ± 8	4.3 ± 1.8

The addition of sorbitol causes a reduction in strength and stiffness but an increment in elongation to break, as expected. Adding a plasticizer increases the free volume by separating the arabinoglucuronoxylan chains from each other and consequently decreasing the hydrogen bonding.

These results proved that flexible arabinoglucuronoxylan films can be prepared without the need of plasticizer. This flexibility is probably due to the side groups that substitute the xylan backbone at 17%.

The mechanical properties of arabinoglucuronoxylan films prevail over the arabinoxylan films previously reported [13].

6.2.2. Dynamic Mechanical Analysis

The measurement of storage modulus in relation to humidity was performed using DMA. The data in Figure 18 illustrate the effect of increasing relative humidity on a arabinoglucuronoxylan sample.

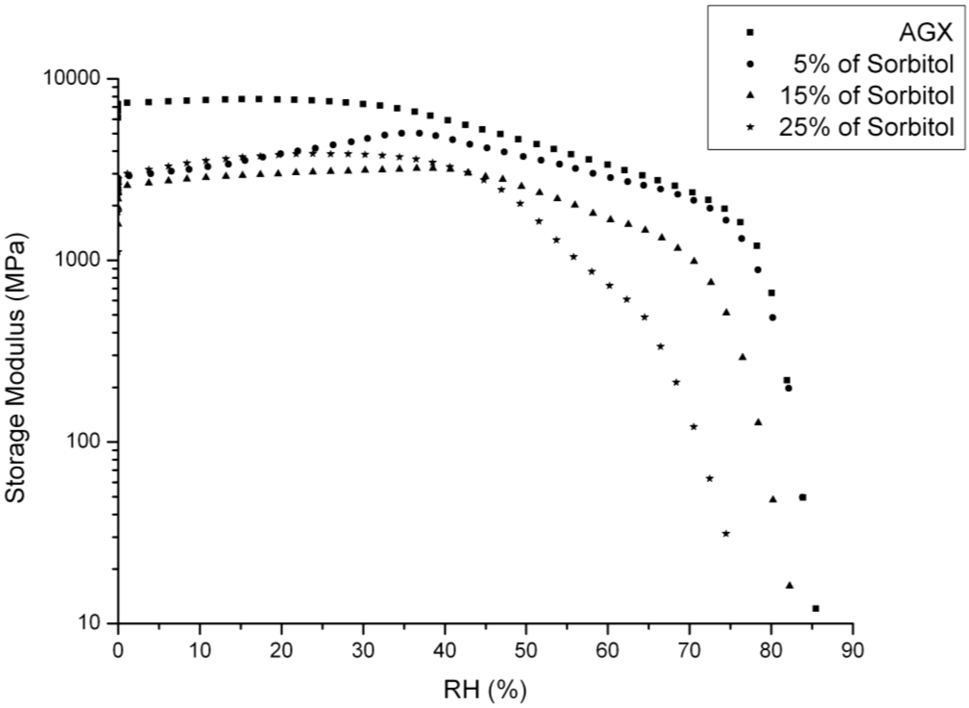

Figure 17 – Humidity scan of arabinoglucuronoxylan films.

As the relative humidity was increased the storage modulus decreased significantly at 80 % RH. The water acts as a plasticizer and reduces the stiffness of the material. These data suggest that even at ambient temperature, the application conditions for arabinoglucuronoxylan films should be maintained below 70% RH to ensure mechanical integrity of the material. Films with the addition of plasticizer softened at a lower relative humidity compared to control films, as was expected. The plasticizers reduces the intermolecular interactions between the chains, thus facilitating interactions between water and the hydroxyl groups of the glucuronic acid side group.

6.3.Barrier Properties

6.3.1. Moisture sorption

Figure 19 shows the water vapour sorption isotherm of the arabinoglucuronoxylan films.

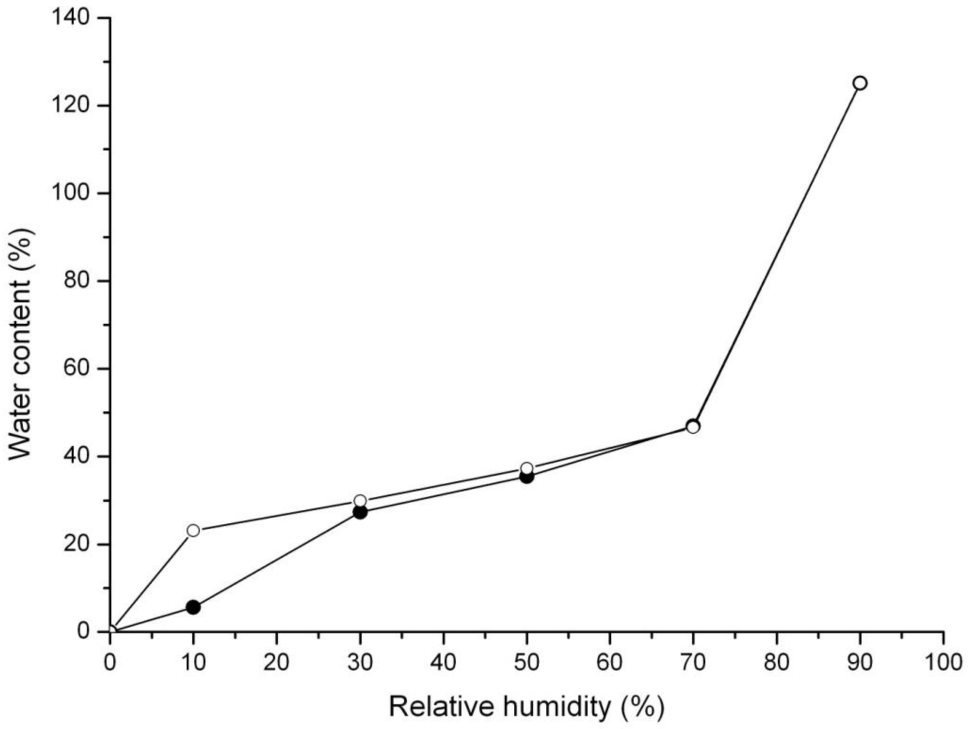

Figure 18 – Water vapour sorption isotherm.

The water content of spruce xylan films increased with the relative humidity, and reached a plateau before it increased again dramatically above 80% RH. This softening behavior corresponds with DMA result where the storage modulus decreases at 80% RH. The water content of arabinoglucuronoxylan at 50% RH was higher than previously reported data for other xylans such as glucuronoxylan from hardwood and arabinoglucuronoxylan from Barley [58]. The hygroscopic nature of arabinoglucuronoxylan is probably due to the fact that the xylan is substituted in both arabinose and glucuronic acid side groups like sodium salt due to extraction. Exchange into acid wood possible contribute to lower moisture content. No hysteresis could be recorded apart from an overall increase in water content at 10% RH that might be due to some rearrangement of the polymer and binding of more water. For polysaccharides a hysteresis in a water isotherm is a common feature at lower RH values as a higher enthalpy of vaporization is needed to remove water molecules sorbed by hydrophilic and charged sites [50].

6.3.2. Oxygen Permeability

The oxygen transmission through arabinoglucuronoxylan films was measured at 50% RH during 5 days and the oxygen permeability was calculated. Table 7 summarizes the oxygen permeability of arabinoglucuronoxylan films and other packaging materials.

Table 7 – Oxygen Permeability of Packaging Material.

Material	**Plasticizer**	**O_2 permeability ($cm^3\ \mu m\ m^{-2}\ d^{-1}\ kPa^{-1}$)**	**Reference**
Arabinoglucuronoxylan	-	0.12 ± 0.07	present study
Arabinoglucuronoxylan	Sorbitol	0.17 ± 0.05	present study
Arabinoxylan	-	0.16	Gröndahl *et al.* [59]
Glucuronoxylan	Sorbitol	0.21	Gröndahl *et al.*[15]
PVA	-	0.19	Gröndahl *et al.*[15]

Arabinoglucuronoxylan film has a low oxygen permeability compared to others barrier plastic materials. It is possible to concluded that arabinoglucuronoxylan films are good oxygen barriers.

7. Conclusion

Hemicellulose was isolated from spruce by Wise and Timell method. NMR spectrum and sugar analysis showed that the spruce xylan is composed mainly of xylose, O-Methyl glucuronic acid and arabinose in a molar ratio 11:2:1, respectively. This value is in agreement with literature values. The Klason lignin content was 16% and the galactoglucomannan content was low (0.6 % w/w). The fraction of the xylan was soluble in $NaNO_3$ solution and had molar mass of 12 780 g/mol. Clear and amorphous films were prepared by water casting.

The unplasticized films were strong with a stress at break above 55 MPa, but quite flexible, with a strain at break around 2.7 %. The Young's Modulus was 2 735 MPa. The stress at break and Young's Modulus of the films decreased, whereas the strain at break increased with increasing sorbitol content. A flexible arabinoglucuronoxylan film can be prepared without the need of plasticizer. The storage modulus of the plasticized films decreased when the surrounding RH was increased in a humidity scan in DMA. The water vapour sorption and the DMA showed that the material is very hygroscopic which is normal for a polysaccharide, which may be because of the side groups. The films exhibited excellent oxygen barrier properties (0.12-0.17 cm^3 μm m^{-2} d^{-1} kPa^{-1}) at 50 % RH. Arabinoglucuronoxylan has a potential in film applications, such as food packaging.

8. Future Work

This work contributes to the knowledge of material and barrier properties of arabinoglucuronoxylan films. Important future work will be to study and improve the water barrier properties of the spruce xylan. The effect of substituent groups on material properties is also an important factor and needs to be investigated.

9. References

1. *APME, The Associations of Plastics Manufaturers in Europe. 2009.*
2. *Marsh, K. and B. Bugusu, Food Packaging—Roles, Materials, and Environmental Issues. Journal of Food Science, 2007.* ***72****(3): p. R39-R55.*
3. *Lange, J. and Y. Wyser, Recent innovations in barrier technologies for plastic packaging—a review. Packaging Technology and Science, 2003.* ***16****(4): p. 149-158.*
4. *Robertson, G., Food Packaging and Shelf Life, in Food Packaging and Shelf Life. 2009, CRC Press. p. 1-16.*
5. *Hartman, J., et al., Oxygen barrier materials from renewable sources: Material properties of softwood hemicellulose-based films. Journal of Applied Polymer Science, 2006.* ***100****(4): p. 2985-2991.*
6. *Bourtoom, T., Edible films and coatings: characteristics and properties. Int. Food Res. J., 2009.* ***16****(Copyright (C) 2011 American Chemical Society (ACS). All Rights Reserved.): p. 237-248.*
7. *Huber, K.C., Embuscado, M.E., Edible Films and Coatings for Food Applications. 2009, Springer New York.*
8. *Sjostrom, E., Wood Chemistry: Fundamentals and Applications. Second ed. 1993: Academic Press. 277.*
9. *Bertaud, F. and B. Holmbom, Chemical composition of earlywood and latewood in Norway spruce heartwood, sapwood and transition zone wood. Wood Sci. Technol., 2004.* ***38****(Copyright (C) 2011 American Chemical Society (ACS). All Rights Reserved.): p. 245-256.*
10. *Suurnäkki, A., et al., Hemicellulases in the bleaching of chemical pulps, in Biotechnology in the Pulp and Paper Industry, K. Eriksson, et al., Editors. 1997, Springer Berlin / Heidelberg. p. 261-287.*
11. *Timell, T.E., Recent progress in the chemistry of wood hemicelluloses. Wood Science and Technology, 1967.* ***1****(1): p. 45-70.*
12. *Willför, S., et al., Polysaccharides in some industrially important softwood species. Wood Science and Technology, 2005.* ***39****(4): p. 245-257.*

13. *Höije, A., et al., Isolation and characterization of physicochemical and material properties of arabinoxylans from barley husks. Carbohydrate Polymers, 2005.* ***61****(3): p. 266-275.*

14. *Sapalidis, A.A., et al., Preparation and characterization of novel poly-(vinyl alcohol)-Zostera flakes composites for packaging applications. Composites Part B: Engineering, 2007.* ***38****(3): p. 398-404.*

15. *Gröndahl, M., L. Eriksson, and P. Gatenholm, Material properties of plasticized hardwood Xylans for potential application as oxygen barrier films. Biomacromolecules, 2004.* ***5****(4): p. 1528-1535.*

16. *Kester, J.J.F., O. R., Edible films and coatings: a review. Food Technology 1986.* ***40****(12): p. 47-59.*

17. *Grondahl, M., A. Gustafsson, and P. Gatenholm, Gas-phase surface fluorination of arabinoxylan films. Macromolecules, 2006.* ***39****(7): p. 2718-2721.*

18. *Peroval, C., et al., Modified arabinoxylan-based films grafting of functional acrylates by oxygen plasma and electron beam irradiation. Journal of Membrane Science, 2004.* ***233****(1-2): p. 129-139.*

19. *Hartman, J., Albertsson, A. C., Lindblad, M. S., Sjoberg, J., Oxygen barrier materials from renewable sources: Material properties of softwood hemicellulose-based films. Journal of Applied Polymer Science, 2006.* ***100****(4): p. 2985-2991.*

20. *Tombs, M.P. and S.E. Harding, An introduction to polysaccharide biotechnology. 1998: Taylor & Francis.*

21. *Ceres. [cited 2011 10 June]; Available from: http://www.ceres.net/Index.html.*

22. *Sjöström, E., Wood chemistry: fundamentals and applications. 1993: Academic Press.*

23. *Marais, S., Enzymatic Hydrolysis with Commercial Enzymes of a Xylan Extracted from Hardwood Pulp, in Department of Chemical Engineering. 2008, University of Pretoria: Pretoria.*

24. *Srndovic, J.S., Interactions between wood polymers in wood cell walls and cellulose/hemicellulose biocomposites. 2011, Chalmers University of Technology: Göteborg.*

25. *Hildén, L., The Characterization of Wood and Wood Fibre Ultrastructure Using Specific Enzymes, in Department of Wood Science. 2004, Swedish University of Agricultural Sciences: Uppsala.*

26. *Chaplin, M. 18 January 2011 [cited 2011 21 February]; Available from: http://www.btinternet.com/~martin.chaplin/hycel.html#fun.*

27. *Resource, R.E. [cited 2011 20 April]; Available from: http://renewableenergyresource.net/cellulosic-ethanol.*

28. *Yaku, F., S. Tsuji, and T. Koshijima, Lignin Carbohydrate Complex. Pt. III. Formation of Micelles in the Aqueous Solution of Acidic Lignin Carbohydrate Complex. Holzforschung, 1979.* ***33****(2): p. 54-59.*

29. *Plomion, C., G. Leprovost, and A. Stokes, Wood Formation in Trees. Plant Physiology, 2001.* ***127****(4): p. 1513-1523.*

30. *Sun, R., X.F. Sun, and J. Tomkinson, Hemicelluloses and Their Derivatives, in Hemicelluloses: Science and Technology. 2003, American Chemical Society. p. 2-22.*

31. *Cai, Z.S. and L. Paszner, Salt Catalyzed Wood Bonding with Hemicellulose. Holzforschung, 1988.* ***42****(1): p. 11-20.*

32. *Porchia, A.C., S.O. Sørensen, and H.V. Scheller, Arabinoxylan Biosynthesis in Wheat. Characterization of Arabinosyltransferase Activity in Golgi Membranes. Plant Physiology, 2002.* ***130****(1): p. 432-441.*

33. *Timell, T.E., Wood Hemicelluloses: Part II, in Advances in Carbohydrate Chemistry, L.W. Melville, Editor. 1965, Academic Press. p. 409-483.*

34. *Ebringerova, A. and T. Heinze, Xylan and xylan derivatives - biopolymers with valuable properties, 1 - Naturally occurring xylans structures, procedures and properties. Macromolecular Rapid Communications, 2000.* ***21****(9): p. 542-556.*

35. *Doner, L.W. and K.B. Hicks, Isolation of hemicellulose from corn fiber by alkaline hydrogen peroxide extraction. Cereal Chemistry, 1997.* ***74****(2): p. 176-181.*

36. *Höije, A., Bioprocessing, Structure and Material Properties of Arabinoxylans, in Department of Chemical and Biological Engineering, Polymer Technology. 2008, Chalmers University of Technology: Göteborg. p. 62.*

37. *Sugawara, M., et al., Composition of Corn Hull Dietary Fiber*

Zusammensetzung der Rohfaser von Maisschalen. Starch - Stärke, 1994. ***46****(9): p. 335-337.*

38. *Félix, G. and T. Zhang, Chiral packing materials for high-performance liquid chromatographic resolution of enantiomers based on substituted branched polysaccharides coated on silica gel. Journal of Chromatography A, 1993.* ***639****(2): p. 141-149.*

39. *Magerstaedt, M., et al., Preparation of polysaccharide ester sulfates as HIV inhibitors. 1991, Hoechst A.-G., Germany . p. 16 pp.*

40. *Saha, B., Hemicellulose bioconversion. Journal of Industrial Microbiology & Biotechnology, 2003.* ***30****(5): p. 279-291.*

41. *Jain, R.K., M. Sjöstedt, and W.G. Glasser, Thermoplastic Xylan Derivatives with Propylene Oxide. Cellulose, 2000.* ***7****(4): p. 319-336.*

42. *Cui, S.W., Food carbohydrates: chemistry, physical properties, and applications. 2005: Taylor & Francis.*

43. *Wyatt, P.J., Light scattering and the absolute characterization of macromolecules. Analytica Chimica Acta, 1993.* ***272****(1): p. 1-40.*

44. *Lifshin, E., Characterization of materials. 1992: VCH.*

45. *Kampf, G., Characterization of Plastics by Physical Methods: Experimental Techniques and Practical Application. 1988: Oxford University Press, USA.*

46. *Faculty, S.T. [cited 2011 25 July]; Available from: http://msc-technology.wikispaces.com/Structures.*

47. *Sepe, M.P., Dynamic Mechanical Analysis for Plastics Engineering. 1998, William Andrew Publishing/Plastics Design Library.*

48. *Williams, C.L.L.D.R., The Characterisation of Pharmaceutical Materials by Dynamic Vapour Sorption. 2006, Surface Measurement Sytems Ltd. p. 4.*

49. *Coultate, T.P., Food: the chemistry of its components. 2000: Royal Society of Chemistry.*

50. *Barbosa-Cánovas, G.V., Water activity in foods: fundamentals and applications. 2007: Blackwell Pub.*

51. *Berk, Z., Food process engineering and technology. 2008: Academic.*

52. *Wise, L.E., M. Murphy, and A.A. Daddieco, Chlorite Holocellulose, Its Fractionation and Bearing on Summative Wood Analysis and on Studies on the Hemicelluloses. Technical Association Papers, 1946.* ***29****(Jun): p. 210-218.*

53. *Timell, T., Isolation of galactoglucomannans from the wood of gymnosperms. Tappi, 1961.* ***44****: p. 88.96.*

54. *Theander, O. and E.A. Westerlund, Studies on Dietary Fiber .3. Improved Procedures for Analysis of Dietary Fiber. Journal of Agricultural and Food Chemistry, 1986.* ***34****(2): p. 330-336.*

55. *Theander, O., et al., Total dietary fiber determined as neutral sugar residues, uronic acid residues, and Klason Lignin (the Uppsala Method): collaborative study. J. AOAC Int., 1995.* ***78****(Copyright (C) 2011 American Chemical Society (ACS). All Rights Reserved.): p. 1030-44.*

56. *Dervilly, G., et al., Isolation and characterization of high molar mass water-soluble arabinoxylans from barley and barley malt. Carbohydrate Polymers, 2002.* ***47****(2): p. 143-149.*

57. *Jacobs, A., et al., Characterization of water-soluble hemicelluloses from spruce and aspen employing SEC/MALDI mass spectroscopy. Carbohydrate Research, 2002.* ***337****(8): p. 711-717.*

58. *Gröndahl, M., A. Teleman, and P. Gatenholm, Effect of acetylation on the material properties of glucuronoxylan from aspen wood. Carbohydrate Polymers, 2003.* ***52****(4): p. 359-366.*

59. *Gröndahl, M. and P. Gatenholm, Oxygen Barrier Films Based on Xylans Isolated from Biomass, in Materials, Chemicals, and Energy from Forest Biomass. 2007, American Chemical Society. p. 137-152.*

Appendix 1

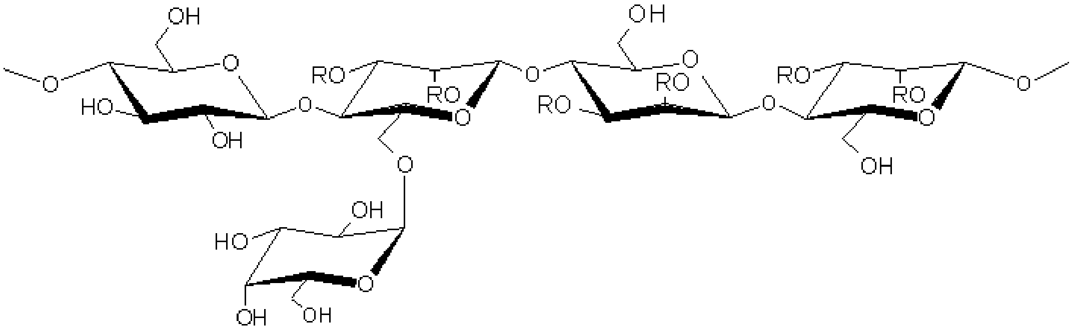

Figure 1 – Principal structure of galactoglucomannans

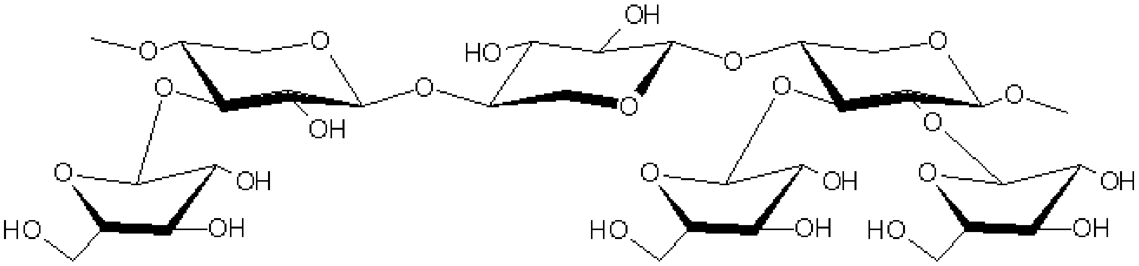

Figure 2 – Abbreviated formula of arabinoxylan

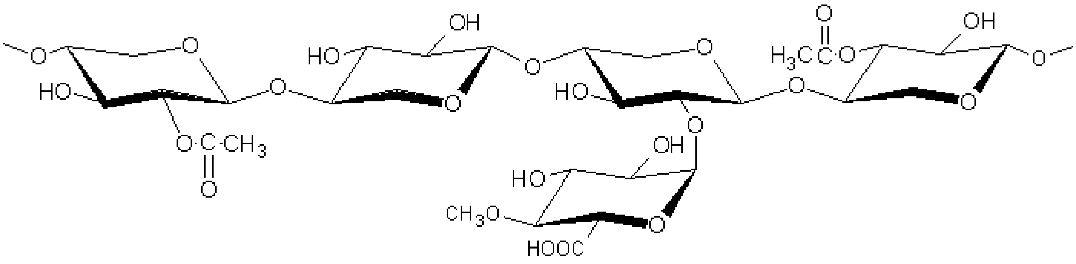

Figure 3 – Abbreviated formula of glucuronoxylan

Appendix 2

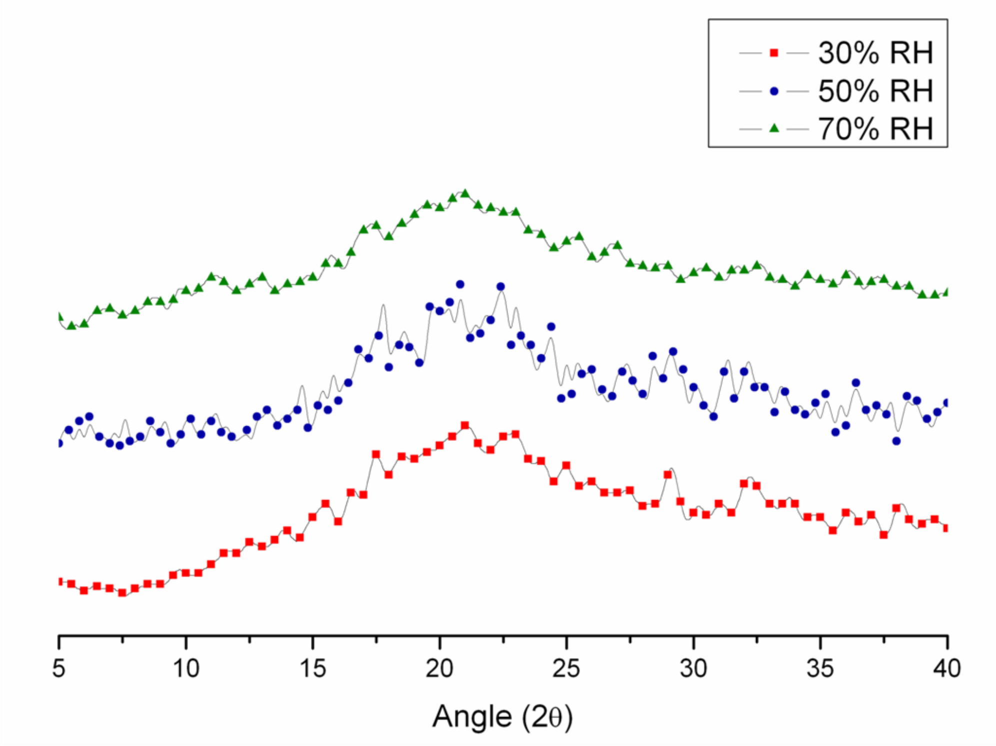

Figure 1 – Diffractograms of arabinoglucuronoxylan films at different dry conditions